HHS Public Access

Author manuscript

*J Mol Cell Cardiol*. Author manuscript; available in PMC 2017 March 01.

Published in final edited form as:

*J Mol Cell Cardiol*. 2016 March ; 92: 10–20. doi:10.1016/j.yjmcc.2016.01.015.

# BAG3 regulates contractility and $Ca^{2+}$ homeostasis in adult mouse ventricular myocytes

**Arthur M. Feldman**[2,3], **Jennifer Gordon**[4], **JuFang Wang**[1], **Jianliang Song**[1], **Xue-Qian Zhang**[1], **Valerie D. Myers**[3], **Douglas G. Tilley**[1], **Erhe Gao**[1], **Nicholas E. Hoffman**[1], **Dhanendra Tomar**[1], **Muniswamy Madesh**[1], **Joseph Rabinowitz**[1], **Walter J. Koch**[1], **Feifei Su**[3,5], **Kamel Khalili**[4], and **Joseph Y. Cheung**[1,2]

[1]Center of Translational Medicine, Temple University School of Medicine, Philadelphia, PA 19140

[2]Department of Medicine, Temple University School of Medicine, Philadelphia, PA 19140

[3]Cardiovascular Research Center, Temple University School of Medicine, Philadelphia, PA 19140

[4]Comprehensive NeuroAIDS Center, Temple University School of Medicine, Philadelphia, PA 19140

[5]Department of Cardiology, Tangdu Hospital, the Fourth Military Medical University, Xi'an, China

## Abstract

Bcl2-associated athanogene 3 (BAG3) is a 575 amino acid anti-apoptotic protein that is constitutively expressed in the heart. BAG3 mutations, including mutations leading to loss of protein, are associated with familial cardiomyopathy. Furthermore, BAG3 levels have been found to be reduced in end-stage non-familial failing myocardium. In contrast to neonatal myocytes in which BAG3 is found in the cytoplasm and involved in protein quality control and apoptosis, in adult mouse left ventricular (LV) myocytes BAG3 co-localized with $Na^+$-$K^+$-ATPase and L-type $Ca^{2+}$ channels in the sarcolemma and t-tubules. BAG3 co-immunoprecipitated with β1-adrenergic receptor, L-type $Ca^{2+}$ channels and phospholemman. To simulate decreased BAG3 protein levels observed in human heart failure, we targeted BAG3 by shRNA (shBAG3) in adult LV myocytes. Reducing BAG3 by 55% resulted in reduced contraction and $[Ca^{2+}]_i$ transient amplitudes in LV myocytes stimulated with isoproterenol. L-type $Ca^{2+}$ current ($I_{Ca}$) and sarcoplasmic reticulum (SR) $Ca^{2+}$ content but not $Na^+/Ca^{2+}$ exchange current ($I_{NaCa}$) or SR $Ca^{2+}$ uptake were reduced in isoproterenol-treated shBAG3 myocytes. Forskolin or dibutyrl cAMP restored $I_{Ca}$ amplitude in shBAG3 myocytes to that observed in WT myocytes, consistent with BAG3 having effects upstream and at the level of the receptor. Resting membrane potential and action potential amplitude were unaffected but $APD_{50}$ and $APD_{90}$ were prolonged in shBAG3 myocytes. Protein levels of $Ca^{2+}$ entry molecules and other important excitation-contraction proteins were

Address correspondence to: Joseph Y. Cheung, M.D., Ph.D., 3401 N. Broad Street, Suite 807, Philadelphia, PA 19140, Joseph.cheung@tuhs.temple.edu, Tel. 215-707-5069, Fax. 215-707-4756.

**Disclosures**

None.

unchanged in myocytes with lower BAG3. Our findings that BAG3 is localized at the sarcolemma and t-tubules while modulating myocyte contraction and action potential duration through specific interaction with the β1-adrenergic receptor and L-type $Ca^{2+}$ channel provide novel insight into the role of BAG3 in cardiomyopathies and increased arrhythmia risks in heart failure.

**Keywords**

BAG3; excitation-contraction coupling; β1-adrenergic receptor; phospholemman; calcium channels

## 1. Introduction

Bcl2-associated athanogene 3 (BAG3) is a stress-activated 575 amino acid protein that is abundantly expressed in the heart, skeletal muscles and many cancers [1]. A member of the 6-member BAG family of proteins, BAG3 regulates protein quality control (PQC) by serving as a co-chaperone of partner proteins including the constitutively and non-constitutively expressed heat shock proteins (Hsc/Hsp) and has anti-apoptotic effects mediated through binding to Bcl2 [1–3]. Recently, it has been shown that BAG3 plays a role in the stability of the sarcomere through regulation of filamin clearance and production and by binding to the actin capping protein beta 1(CapZβ1), a sarcomere protein that binds to the barbed end of actin to prevent its disassociation into actin monomers [4, 5].

The notion that BAG3 plays an important role in cardiovascular pathophysiology was first demonstrated by the finding that mice with homozygous deletion of the BAG3 gene had postnatal deterioration with death by 4 weeks of age due to non-inflammatory myofibrillar degeneration [6]. Subsequently, functional mutations in BAG3 were found in childhood-onset muscular dystrophy with involvement of skeletal, respiratory and cardiac muscles [7, 8], in families with dilated cardiomyopathy but without neuropathy or peripheral muscle weakness [9, 10], and in sporadic cases of idiopathic dilated cardiomyopathy [11]. In addition, BAG3 protein levels in hearts from patients with end-stage heart failure (HF) but without BAG3 mutations were significantly less than those measured in non-failing control hearts, suggesting that decreased levels of BAG3 might contribute to the pathophysiology of both familial and non-familial HF [9].

The function and regulation of BAG3 in the heart remains largely unexplored. Knockdown of BAG3 in neonatal myocytes led to disruption of myofibril structures and CapZβ1 ubiquitin-proteasome-mediated degradation in the presence of mechanical stress, suggesting that BAG3 plays a role in PQC and helps maintain the structural integrity of the contractile elements [12]. However, several findings suggest that BAG3 may play a larger role in myocardial biology. For example, disruption of myofibril structures was not a ubiquitous finding in patients with mutations in BAG3 and idiopathic dilated cardiomyopathy [13], and giant axonal neuropathy and neural conduction velocity slowing were found in affected members of a family with a BAG3 mutation and hypertrophic cardiomyopathy [14]. Therefore, the current study was undertaken to test the hypothesis that BAG3 can influence myocyte contractility in adult cardiac myocytes. We report for the first time that in contrast to neonatal myocytes, BAG3 is localized predominantly in the sarcolemma and t-tubules of

adult cardiac myocytes and modulates myocyte contraction in response to β-adrenergic receptor signaling. Thus, BAG3 plays an important role in regulation cardiac contractile function in addition to its effects on protein quality control.

## 2. Materials and methods

### 2.1. Construction of Adv-BAG3-shRNA

BAG3shRNA-Ad construct was made using the BD Adeno-X Expression Systems 2PT3674-1 (Pr36024) and BD knockout RNAi Systems PT3739 (PR42756)(BD Biosciences-Clontech, Palo Alto, CA) as previously described [15]. A dsDNA oligonucleotide against a specific BAG3 mRNA (5′-AAG GUU CAG ACC AUC UUG GAA-3′) was inserted in a RNAi-ready pSIREN-DNR vector designed to express a small hairpin RNA (shRNA) driven by the human Pol III-dependent U6 promoter. After ligation, this vector was used to transfer the shRNA expression cassette to the Adenoviral Acceptor Vector pLP-Adeno-X-PRLS viral DNA (BD Adeno-X Expression Systems 2) containing ΔE1/ΔE3 Ad5 genome by Cre-loxP mediated recombination. An AdNull empty adenoviral vector was used as control. Adenoviruses were propagated in a HEK-293 cell line, purified and titered (plaque-forming unit; pfu) according to standard techniques.

### 2.2. Isolation of adult murine cardiac myocytes

Cardiac myocytes were isolated from the septum and LV free wall of C57BL/6 mice (10–12 wks old) according to the protocol of Zhou et al. [16], and plated on laminin-coated glass coverslips [17]. Coverslips containing myocytes were mounted in Dvorak-Stotler chamber, and bathed in fresh media before measurements.

### 2.3. Preparation of neonatal rat ventricular myocyte (NRVM) and neonatal mouse ventricular myocyte (NMVM) cultures

Primary NRVM cultures were prepared from 1–2 day old Sprague Dawley rat pups by enzymatic digestion as described previously [18]. Briefly, hearts were excised and placed in sterile solution containing (in mM): NaCl 116, HEPES 20, $Na_2HPO_4$ 0.08, glucose 5.6, KCl 5.4, $MgSO_4.7H_2O$ 0.8; pH 7.35. Ventricles were minced and subjected to 5 × 15 min enzymatic digestions using collagenase II and pancreatin. NRVMs were separated from fibroblasts via pre-plating for 2 h and cultured overnight in F-10 media containing 10% horse serum, 5% fetal bovine serum (FBS) and 1% penicillin:streptomycin:fungizone (PSF) at 37°C in a humidified incubator with 5% $CO_2$. The following day, media was replaced with F-10 media containing 5% FBS and 1% PSF. NRVMs were cultured for 24 h in MEM containing 10% FBS and 1% PSF at 37°C in a humidified incubator with 5% $CO_2$. After 24 h the media was replaced with 5% FBS-containing media.

Primary NMVM cultures were prepared from 1–2 day old FVB mouse pups using Pierce Primary Cardiomyocyte Isolation Kit (#88281; Thermo Scientific, Rockford, IL) according to manufacturer's instructions. Briefly, neonatal hearts were minced and digested with two combined enzyme suspensions. Upon removal of enzyme solution the tissue was washed repeatedly with ice-cold Hank's Buffered Salt Solution. After washing, Dulbecco's Modified Eagle Medium (DMEM) was added and used to break up the tissue into cells.

Once a single-cell suspension was achieved more DMEM was added and individual suspensions were combined to determine cell concentration and cell viability. NMVMs were cultured in DMEM with Cardiomyocyte Growth Supplement at 37°C and 5% $CO_2$.

### 2.4. Immunolocalization of BAG3 in adult LV myocytes and neonatal ventricular myocytes

Freshly isolated WT mouse LV myocytes adherent to laminin-coated coverslips were washed 3x with phosphate buffered saline containing 2 mM EGTA (PBS-E). Adult LV myocytes and neonatal ventricular myocytes were fixed for 30 min in 4% paraformaldehyde in PBS-E. After 2 rinses with PBS-E, myocytes were permeabilized for 2 min with 0.05% Triton X-100. Myocytes were rinsed 2x with PBS-E, and once with BLOTTO (5% nonfat dry milk, 0.1 M NaCl, and 50 mM Tris.HCl; pH 7.4). Primary antibodies against BAG3 (1:50; Proteintech Group Inc, Chicago, IL) diluted in BLOTTO were added to the cells, incubated at room temperature in the dark for 60 min, and rinsed 3x with BLOTTO. Secondary antibodies (Alexafluor 594-labeled goat anti-rabbit IgG; 1:50; Invitrogen, Eugene, OR) diluted in BLOTTO were added to the cells, incubated in the dark for 30 min, and followed by 3 PBS-E rinses. $Na^+$-$K^+$-ATPase was detected with Alexafluor 488-labeled anti-α1 subunit antibody (1:250; Millipore; ex. 488 nm, em. 510 nm). L-type $Ca^{2+}$ channels were detected with anti-α1c-$Ca_V$1.2 antibody (1:250, Millipore; secondary antibody Alexafluor 488-labeled goat anti-rabbit IgG). Coverslips were mounted to slides with Prolong Gold Anti-fade mounting solution (Invitrogen). Confocal images (63× oil objective; 510 Meta; Carl Zeiss, Inc.) were acquired at 594 nm excitation and 617 nm emission for BAG3.

### 2.5. Knockdown of BAG3 by Adv-shRNA BAG3 injection into LV

After cleansing the skin with betadine solution, the left chest of anesthetized (2% inhaled isoflurane) mouse was opened, the heart exteriorized, and 35 μl (total volume) of Adv-GFP ($3.3 \times 10^8$ pfu) or Adv-shRNA BAG3 ($7.5 \times 10^7$ pfu) was directly injected to anterior and posterior LV wall and the apex. Since Adv-shRNA BAG3 does not encode GFP, Adv-GFP was mixed with Adv-shRNA BAG3 before injection. The heart was returned to the chest cavity and the wound sutured. The entire surgical procedure took <45 seconds. Typically >95% of animals survived the procedure. Survivors were allowed to recover for 10 days before hearts were excised and myocytes (GFP and shBAG3) were isolated from areas of LV that fluoresced green [19].

### 2.6. Measurement of $[Ca^{2+}]_i$ and contraction in cardiac myocytes

Fura-2 loaded (0.67 μM fura-2 AM, 15 min) myocytes adherent to laminin-coated coverslips were incubated in HEPES-buffered (20 mM, pH 7.4) medium 199 (1.8 mM $[Ca^{2+}]_o$) and field stimulated to contract (2 Hz; 37°C). Myocytes were exposed to excitation light (360 and 380 nm) only during data acquisition. Epifluorescence (510 nm) was measured in steady-state twitches both before and after addition of isoproterenol (Iso; 1 μM)[17, 19–23]. For contraction measurements, images of myocytes (not loaded with fura-2) were captured by a charge coupled device video camera and myocyte motion was analyzed offline with edge detection algorithm [17, 19–23].

### 2.7. $I_{NaCa}$, $I_{Ca}$, SR $Ca^{2+}$ content and AP measurements

Whole cell patch-clamp recordings were performed at 30°C as described previously [17, 24]. Pipette diameter was 4 – 6 μm and pipette resistance was 0.8 to 1.4 MΩ when filled with standard internal solution. $I_{Ca}$, $I_{NaCa}$ and SR $Ca^{2+}$ contents were normalized to membrane capacitance ($C_m$) before comparison between GFP and shBAG3 myocytes.

For $I_{NaCa}$ measurements, pipette solution contained (in mM): $Cs^+$-glutamate 100, $Na^+$-HEPES 7.25, $MgCl_2$ 1, HEPES 12.75, $Na_2ATP$ 2.5, EGTA 10, and $CaCl_2$ 6; pH 7.2. Free $Ca^{2+}$ in the pipette solution was 205 nM. Myocytes were bathed in an external solution containing (in mM): NaCl 130, CsCl 5, $MgSO_4$ 1.2, $NaH_2PO_4$ 1.2, $CaCl_2$ 5, HEPES 10, $Na^+$-HEPES 10, and glucose 10; pH 7.4 [25–27]. Verapamil (1 μM) was added to block L-type $Ca^{2+}$ currents. The myocyte was held at the calculated equilibrium potential for $I_{NaCa}$ ($E_{NaCa}$) of −73 mV for at least 5 min before current was elicited with a descending-ascending voltage ramp (from +100 to −120 and back to +100 mV, 500 mV/s). $I_{NaCa}$ was defined as the difference current in the absence and presence of $NiCl_2$ (1 mM). Our conditions for measuring $I_{NaCa}$ were carefully chosen to minimize contamination by $Na^+$-$K^+$-ATPase activity ($K^+$-free) and ion fluxes through the $Na^+/Ca^{2+}$ exchanger before the onset of voltage ramp (by holding the cell at the calculated $E_{NaCa}$), thereby allowing $[Na^+]_i$ and $[Ca^{2+}]_i$ to equilibrate with those present in the pipette solution [25].

For $I_{Ca}$ measurements, pipette solution contained (in mM): CsCl 110, TEA.Cl 20, HEPES 10, MgATP 5, and EGTA 10; pH 7.2. Extracellular bathing solution contained (in mM): N-methyl-D-glucamine 137, CsCl 5.4, $CaCl_2$ 2, $MgSO_4$ 1.3, HEPES 20, 4-aminopyridine 4, and glucose 15; pH 7.4. Holding potential was at −90 mV [28]. To ensure steady-state SR $Ca^{2+}$ loading, 6 conditioning pulses (from −70 to 0 mV, 100 ms, 2 Hz) were delivered to the myocyte before the arrival of each test pulse (from −90 to +50 mV, 10 mV increments, 60 ms)[28]. Leak-subtracted inward currents were used in analysis for $I_{Ca}$ amplitudes and inactivation kinetics. Inward currents obtained under these conditions were blocked by 1 μM verapamil (data not shown).

SR $Ca^{2+}$ content was estimated by integrating forward $I_{NaCa}$ induced by caffeine exposure [29, 30]. The pipette solution consisted of (in mM): $Cs^+$-glutamate 100, $MgCl_2$ 1, HEPES 30 and MgATP 2.5, pH 7.2. The external solution contained (in mM): NaCl 130, CsCl 5, $MgSO_4$ 1.2, $NaH_2PO_4$ 1.2, $CaCl_2$ 1.8, HEPES 20, glucose 10, pH 7.4; 30°C. Holding potential was −90 mV. At 200ms after the $12^{th}$ conditioning pulse (from −90 to 0 mV, 300ms, 1 Hz), with membrane potential held at −90 mV, caffeine (5 mM, 2.4s) was applied. The resulting large transient inward current (digitized at 0.5 kHz and collected for 5s) represents $Na^+$ entry accompanying $Ca^{2+}$ extrusion by $Na^+/Ca^{2+}$ exchanger, and $t_{1/2}$ of $I_{NaCa}$ decline is a functional readout of $Na^+/Ca^{2+}$ exchange activity. The time integral of this current is an estimate of SR releasable $Ca^{2+}$. To convert $I_{NaCa}$ time integral (coulombs) to moles, charge was divided by Faraday's constant of 96,487 coulombs/equivalent, based on 3 $Na^+$ being exchanged for each $Ca^{2+}$.

For AP measurements, myocytes were paced at 1 Hz. Pipette solution consisted of (in mM): KCl 125, $MgCl_2$ 4, $CaCl_2$ 0.06, HEPES 10, $K^+$-EGTA 5, $Na_2ATP$ 3, and $Na_2$-creatine phosphate 5, (pH 7.2). External solution consisted of (in mM): NaCl 132, KCl 5.4, $CaCl_2$

1.8, $MgCl_2$ 1.8, $NaH_2PO_4$ 0.6, HEPES 7.5, $Na^+$-HEPES 7.5, and glucose 5, pH 7.4. APs were recorded using the current clamp configuration at 1.5x threshold stimulus, 4-ms duration, and 30°C [31].

### 2.8. Immunoblotting

Mouse LV homogenates were prepared as previously described [17]. Gradient (4–12%) gels were used in all Western blots. For detection of BAG3, $\alpha_1$- and $\alpha_2$-subunits of $Na^+$-$K^+$-ATPase, $\alpha_{1c}$-subunit of L-type $Ca^{2+}$ channel ($Ca_v1.2$), sarco(endo)plasmic reticulum $Ca^{2+}$-ATPase (SERCA2), calsequestrin, cardiac ryanodine receptor (RyR2), RyR2 phosphorylated at serine$^{2808}$ or serine$^{2814}$ ($p^{2808}$RyR2 and $p^{2814}$RyR2, respectively), reducing conditions (5% β-mercaptoethanol) was used. For detection of $Na^+/Ca^{2+}$ exchanger (NCX1), non-reducing conditions (10 mM N-ethylmaleimide) were used. Antibodies for α1- and α-2 subunits of $Na^+$-$K^+$-ATPase, SERCA2, NCX1, $\alpha 1_c$-subunit of $Ca_v1.2$ and calsequestrin were sourced and used as described previously [17, 19–23]. RyR2 and its phosphorylated forms were detected with anti-RyR2 (1:1,000; Thermo Scientific), anti-$p^{2808}$RyR2 (1:1,000; Abcam, Cambridge, MA) and anti-$p^{2814}$RyR2 (1:5,000; Badrilla, Leeds, UK) antibodies. Blots were washed and incubated with appropriate secondary antibody conjugated to horse radish peroxidase. Enhanced chemiluminescence (ECL, Amersham) was used for the detection of signals.

### 2.9. Co-immunoprecipitation

Two hours after isolation, mouse LV myocytes were infected with Adv-GFP ($6.6 \times 10^7$ pfu/ml) or Adv-GFP-myc-tagged human BAG3 ($1.1 \times 10^7$ pfu/ml) + Adv-β1AR-HA ($1.65 \times 10^6$ pfu/ml) in 1 ml of FBS-free Eagle's minimal essential media (MEM) containing (in mM): creatine 5, carnitine 2, taurine 5, 2,3-butanedione monoxime (BDM) 10, $NaHCO_3$ 4.2, 0.2 % bovine serum albumin, penicillin (30 mg/L), gentamicin (4 mg/L) and insulin-transferrin-selenium supplement for 3h. One additional ml of MEM (with same supplements) was then added, and myocytes were cultured for 48h. Media was changed daily. Cultured myocytes were scraped into lysis buffer [in mM: Tris 50 (pH 8.0), NaCl 150, $Na^+$ orthovanadate 1, PMSF 1, NaF 100, EDTA 1 and EGTA 1 with 0.5% NP-40, 10 μg/ml leupeptin and 10 μg/ml aprotinin], sonicated and centrifuged at 10,000rpm and 4°C for 10 min. 40ul (50% slurry) monoclonal anti-HA-agarose beads were added to 600μl of supernatant (400 μg protein) and incubated overnight on a rotating platform at 4°C. Beads were pelleted and washed 4x with 1ml ice-cold PBS. 52 ul of 2x loading buffer were added to the beads, and incubated at room temperature for 30 min with slow vortex every 5 min. The bead suspension was centrifuged at 5000g for 1 min and 40 μl of the supernatant were collected. Supernatant was heated at 70°C for 5 min before immunoblotting (7.5% SDS-PAGE, reducing conditions with 5% β-mercaptoethanol). Blots were incubated with primary anti-HA antibody (1:1,000) followed by anti-mouse secondary antibody (1:15,000; Li-Cor). Potential co-immunoprecipitates of interest were detected by anti-BAG3 (1:1,000), anti-α1c-$Ca_v1.2$ (1:200), anti-α1-$Na^+$-$K^+$-ATPase (1:1,000); anti-PLM (C2, 1:1,000), anti-Hsp70 (1:500) and anti-CapZβ1 (1:500) antibodies. Protein band signals were detected by Li-Cor.

To detect association between endogenous BAG3 and $Ca_v1.2$, freshly isolated mouse LV myocytes were placed in 300 μl of ice-cold Buffer I [in mM: Tris 10 (pH 7.5), $Na^+$ vanadate

1, PMSF 1, NaF 100, EGTA 1, and a combination of complete protease inhibitor (Roche Diagnostics; Indianapolis, IN), phosphatase inhibitor cocktails (Sigma) and $C_{12}E_8$ (5 mg/ml)]. Myocyte lysates were precleared with protein A agarose for 3h at 4°C. Precleared supernatants were incubated with either 10 μg of preimmune rabbit IgG, anti-BAG3, or anti-α1c-$Ca_v$1.2 antibodies overnight at 4°C. The next day, 40 μl (50% slurry) of washed, suspended protein A agarose beads were added to each sample and incubated for a further 2h at 4°C. Beads were pelleted, washed 6x with 1.5 ml of ice-cold PBS, and resuspended in 50 μl of 2x Laemmli sample buffer (+ β-mercaptoethanol). Beads were extracted as described above, and immunoblotting was performed.

### 2.10. Statistics

All results are expressed as means ± SE. For analysis of $[Ca^{2+}]_i$ transient and contraction amplitudes, and SR $Ca^{2+}$ contents as a function of group and Iso; $I_{NaCa}$ and $I_{Ca}$ as a function of group and voltage, two-way ANOVA was used. For analysis of action potential parameters, $C_m$ and protein abundance, one-way ANOVA was used. A commercially available software package (JMP version 12; SAS Institute, Cary, NC) was used. In all analyses, $p<0.05$ was taken to be statistically significant.

## 3. Results

### 3.1. BAG3 is localized in sarcolemma and t-tubules in adult mouse LV cardiac myocytes

Loss of cardiac BAG3 expression in both the adult heart and neonatal cardiac myocytes has been associated with structural disorganization, but little is known about the localization or functional impact of endogenous BAG3 in cardiac myocytes. In freshly isolated adult mouse LV myocytes. BAG3 was expressed in sarcolemma and t-tubules (Fig. 1A, left panel) and co-localized with $Na^+$-$K^+$-ATPase (Fig. 1B) and L-type $Ca^{2+}$ channels (Fig. 1C). By contrast, in NRVMs (Fig. 1A, middle panel) and NMVMs (Fig. 1A, right panel), BAG3 was expressed diffusely in the cytoplasm.

### 3.2. BAG3 associates with β1-adrenergic receptor, L-type $Ca^{2+}$ channel and phospholemman in adult LV myocytes

BAG3 expression in the sarcolemma and t-tubules of adult cardiac myocytes supports a possible role in the regulation of contractile events, thus we further explored whether BAG3 associates with key mediators of cardiac myocyte contractility. In adult myocytes expressing both β1AR-HA and BAG3-myc, anti-HA antibody immunoprecipitated not only β1AR-HA but also BAG3, $Ca_v$1.2 and phospholemman (PLM), but not $Na^+$-$K^+$-ATPase (Fig. 2A). PLM, which belongs to the FXYD family of ion transport regulators [32], is expressed in the sarcolemma and t-tubules of adult cardiac myocytes [33] and regulates $Na^+$-$K^+$-ATPase [34], $Na^+/Ca^{2+}$ exchanger [33] and L-type $Ca^{2+}$ channel [28]. We could not detect association between BAG3 and Hsp70 (Fig. 2B). Association between BAG3 and CapZβ1 was indeterminate since the signal was present in both control myocytes expressing GFP and myocytes expressing β1AR-HA/BAG3-myc (Fig. 2B). In freshly isolated and non-infected mouse LV myocytes, immunoprecipitating endogenous BAG3 brought down $Ca_v$1.2 while immunoprecipitating $Ca_v$1.2 brought down BAG3 (Fig. 2C).

### 3.3. BAG3 downregulation depresses myocyte contractility and reduces $[Ca^{2+}]_i$ transient amplitudes

Since BAG3 associates with upstream modulators of contraction, but its levels are decreased in heart failure, we undertook to evaluate the impact of loss of endogenous BAG3 on adult cardiac myocyte contractility. To simulate reduced BAG3 protein levels in HF [1, 9], we downregulated BAG3 by injecting Adv-shRNA BAG3 ($7.5 \times 10^7$ pfu in 10 μl) + Adv-GFP ($3.3 \times 10^8$ pfu in 25 μl) in intact myocardium while hearts injected with Adv-GFP served as controls [35]. Ten days after virus injection, myocytes were isolated from the areas of LV that exhibited GFP fluorescence. BAG3 levels significantly decreased in shBAG3 compared to GFP myocytes (Fig. 3A; Table 1). BAG3 knockdown did not alter expression of $\alpha_1$- and $\alpha_2$-subunits of $Na^+$-$K^+$-ATPase, $Na^+/Ca^{2+}$ exchanger, $\alpha_{1c}$-subunit of $Ca_v1.2$, total RyR2, phosphorylated RyR2 and SERCA2 (Fig. 3A; Table 1). In addition, there were no significant differences ($p<0.6$) in cell sizes as reflected by similar whole cell capacitance ($C_m$, a measure of cell surface area) between GFP (163.1 ± 5.4 pF; n=20 myocytes from 7 mice) and shBAG3 (167.7 ± 5.7 pF; n=22 myocytes from 7 mice) myocytes.

$[Ca^{2+}]_i$ transient amplitudes were similar at baseline but were significantly lower in shBAG3 compared to control GFP myocytes after isoproterenol (Fig. 3B; Table 2; group x iso interaction effect, $p<0.03$). Likewise, single myocyte contraction amplitudes were similar at baseline but significantly reduced in shBAG3 compared to GFP myocytes after isoproterenol (Fig. 3C; Table 2; group x iso interaction effect, $p<0.01$). There were no differences in $t_{1/2}$ of $[Ca^{2+}]_i$ transient decline (Table 2), suggesting similar SR $Ca^{2+}$ uptake rates between GFP and shBAG3 myocytes and consistent with the observation that SERCA2 expression did not change with BAG3 downregulation (Fig. 3A).

### 3.4. Effects of BAG3 downregulation on $I_{NaCa}$, $I_{Ca}$, SR $Ca^{2+}$ contents and APD

The major determinants of $[Ca^{2+}]_i$ transient amplitude are the triggers for SR $Ca^{2+}$ release ($I_{Ca}$ and reverse $I_{NaCa}$) and SR $Ca^{2+}$ content. Since $I_{NaCa}$ was not affected by isoproterenol in adult rodent cardiac myocytes [27, 36, 37], we measured $I_{NaCa}$ at baseline and found no differences between GFP and shBAG3 myocytes (Fig. 4A). Under basal conditions, maximal $I_{Ca}$ amplitude and voltage at which $I_{Ca}$ peaked were similar in GFP and shBAG3 myocytes (Fig. 4B). The inactivation time constant of $I_{Ca}$ measured at −10 mV ($\tau_{inact}$) was similar between GFP (12.2 ± 0.8 ms; n=12 myocytes from 5 mice) and shBAG3 myocytes (13.3 ± 0.63 ms; n=21 from 9 mice)($p<0.3$). By contrast, in the presence of isoproterenol, maximal $I_{Ca}$ amplitude was significantly ($p<0.02$; group x Iso interaction effect) lower in shBAG3 myocytes (Fig. 4B; Table 3) but $\tau_{inact}$ was similar between GFP (8.0 ± 0.7 ms; n=5 myocytes from 3 mice) and shBAG3 (10.0 ± 1.5 ms; n=8 myocytes from 5 mice)($p<0.25$) myocytes. To determine if the shBAG3-mediated decrease in responsiveness to Iso was due to a generalized defect in cAMP signaling, we directly activated adenylyl cyclase (forskolin) or protein kinase A (dibutyryl cAMP). Addition of either forskolin (10 μM) or dibutyryl cAMP (5 mM) produced maximal $I_{Ca}$ amplitudes in shBAG3 myocytes that were not different than those observed in GFP myocytes stimulated with Iso (Table 3). SR $Ca^{2+}$ contents were not different between GFP and shBAG3 myocytes at baseline but were lower in shBAG3 myocytes in the presence of isoproterenol (Fig. 4C; Table 2). In addition, $t_{1/2}$ of $I_{NaCa}$ decline after caffeine-induced SR $Ca^{2+}$ release was similar between GFP and shBAG3

myocytes (Fig. 4C; Table 2), in agreement with no differences in $I_{NaCa}$ measured in GFP and shBAG3 myocytes (Fig. 4A).

Finally, resting membrane potential and action potential amplitude were similar between GFP and shBAG3 myocytes, both in the absence and presence of isoproterenol (Fig. 5). BAG3 downregulation resulted in prolongation of $APD_{50}$ ($p<0.03$) and $APD_{90}$ ($p<0.05$) (Fig. 5), both in the absence and presence of isoproterenol.

## Discussion

BAG3 is constitutively expressed in the heart and skeletal muscle and to a lesser extent in organs containing extensive smooth muscle including the uterus, bladder and aorta [2, 3]. Little is known regarding the function of BAG3 in the adult heart. Four lines of evidence suggest that BAG3 is likely to play a significant role in the pathobiology of HF: (i) mice in which BAG3 was knocked out developed non-inflammatory myofibrillar degeneration, disruption of Z-disk architecture and apoptotic features in the early postnatal period and death by 4 weeks of age [6]; (ii) BAG3 mutations are associated with familial dilated cardiomyopathy [7–11, 38]; (iii) knockdown of BAG3 in neonatal myocytes resulted in significant cardiac dysfunction and myofibrillar degeneration in response to stress [12]; and (iv) myocardial levels of BAG3 were substantially reduced in hearts from patients with non-heritable forms of HF and in animal models of HF [1]. The present study demonstrates for the first time that in adult cardiac myocytes, BAG3 facilitates the ability of β-adrenergic signaling to augment cardiac contraction through alterations in $Ca^{2+}$ homeostasis – a finding that has important implications for our understanding of excitation-contraction coupling in the heart.

The first major finding is that in contrast to NRVMs and NMVMs, confocal imaging demonstrated BAG3 in the sarcolemma and t-tubules, with little-to-no signal in the sarcoplasm of adult mouse cardiac myocytes. This observation was supported by the finding that BAG3 associated with β1 adrenergic receptor, L-type $Ca^{2+}$ channels and phospholemman but not $Na^+$-$K^+$-ATPase and is consistent with previous reports that there is a separate pool of phospholemman that does not regulate or associate with the $Na^+$ pump [39]. The marked differences between BAG3 localization in neonatal and adult cardiac myocytes is consistent with the observation in cardiomyoblasts that the functional role of BAG3 changes with different developmental stages [40].

The second major finding is that adenoviral delivery of shRNA-BAG3 was efficacious in knocking down BAG3 levels by ~54% in adult mouse hearts after 10 days of infection – a decrease comparable to that seen in human hearts with end-stage failure and in animal models of HF [1]. We have recently reported that BAG3 levels were unchanged after 2 days of Adv-shRNA-BAG3 infection [35], suggesting that the turnover of BAG3 in adult mouse myocytes is relatively slow.

The third substantive observation is that BAG3 downregulation to ~50% of that found in normal WT myocytes resulted in reduced maximum contraction amplitude in response to βAR stimulation, an effect that was not associated with myocyte hypertrophy (similar $C_m$) or

altered expression levels of protein involved in $Ca^{2+}$ dynamics. These results suggest that BAG3 plays a critical role in modulating cardiac response to catecholamines.

To understand the mechanism responsible for alterations in myocyte contractility, we investigated changes in $Ca^{2+}$ homeostasis in single myocytes. The major determinants of $[Ca^{2+}]_i$ transient amplitude are the trigger for SR $Ca^{2+}$ release ($I_{Ca}$ and reverse $I_{NaCa}$), the gain of ryanodine receptor, and SR $Ca^{2+}$ content. BAG3 downregulation resulted in decreased $I_{Ca}$ and SR $Ca^{2+}$ contents in myocytes treated with isoproterenol. However, $I_{Ca}$ was not reduced in shBAG3 myocytes exposed to either forskolin or dbcAMP, suggesting defects in β-adrenergic receptor signaling occurred proximal to adenylyl cyclase. This conclusion is given circumstantial support in that BAG3, β1AR and L-type $Ca^{2+}$ channel physically associated with each other and likely formed a macromolecular signaling complex in adult cardiac myocytes. Decreased SR $Ca^{2+}$ content in shBAG3 myocytes was not due to reduced SR $Ca^{2+}$ uptake since SERCA2 expression was not affected by BAG3 downregulation and SR $Ca^{2+}$ uptake activity, as reflected by $t_{1/2}$ of $[Ca^{2+}]_i$ transient decline [29], was similar between GFP and shBAG3 myocytes. The lower SR $Ca^{2+}$ content in shBAG3 myocytes exposed to isoproterenol may be due to decreased SR $Ca^{2+}$ loading by $I_{Ca}$ (but not by reverse $I_{NaCa}$). Although RyR2 phosphorylation was not affected by BAG3 downregulation, our study did not go into sufficient depth to exclude enhanced SR $Ca^{2+}$ leak as contributing to decreased SR $Ca^{2+}$ content in shBAG3 myocytes.

The molecular mechanism by which β-adrenergic agonist stimulates $I_{Ca}$ is incompletely elucidated. A definitive understanding of where, if and how the $Ca_v1.2$ protein complex is phosphorylated in response to β-adrenergic receptor stimulation to increase $I_{Ca}$ remains stubbornly elusive [41]. To account for our observation that isoproterenol-induced increase in $I_{Ca}$ but not SR $Ca^{2+}$ uptake was blunted in shBAG3 myocytes, we propose that there is a specific pool of β1AR that complexes with BAG3 and $Ca_v1.2$ and facilitates β1-adrenergic signaling to increase $I_{Ca}$. With BAG3 knockdown, the pool of β1AR-BAG3-$Ca_v1.2$ macromolecular complex is decreased and therefore accounts for the diminished $I_{Ca}$ in Iso-treated shBAG3 myocytes. Another pool of β1AR that is not complexed with BAG3 and $Ca_v1.2$ stimulates SR $Ca^{2+}$ uptake by phosphorylating phospholamban. The notion that there are separate pools of the same protein is not without precedent since that there are different pools of phospholemman, one pool associates with $Na^+$ pump while the other pool does not [39].

An unexpected finding was that BAG3 downregulation resulted in AP prolongation in myocytes, regardless of whether they had been treated with isoproterenol. Since AP morphology and duration are largely dependent on voltage-dependent ion currents, AP prolongation provides additional support that BAG3 modulated sarcolemmal ion channel activity. In addition, since cell sizes were similar between GFP and shBAG3 myocytes, altered AP morphology is a primary effect of BAG3 downregulation rather than a secondary effect associated with myocyte hypertrophy. Since AP prolongation is associated with increased risks of arrhythmias, BAG3 reduction may account for increased risks of sudden death in patients with familial dilated cardiomyopathy and patients with end-stage heart failure.

In summary, BAG3 is expressed at the sarcolemma and t-tubules of adult cardiac myocytes, regulates ion channel activities, modulates β-adrenergic receptor signaling and action potential duration. BAG3 regulates cardiac contractility by affecting excitation-contraction coupling in adult cardiac myocytes. Viewed in the context that both familial dilated cardiomyopathy and end-stage heart failure are associated with reduced BAG3 protein levels, BAG3 represents a novel therapeutic target in the treatment of human heart failure. While earlier studies suggested that a major function of BAG3 in the heart is to improve protein quality control and stabilize the contractile proteins [1], the present study demonstrates that a fundamental effect of enhanced levels of BAG3 might also be improved β-adrenergic signaling, enhanced cardiac performance and reduced arrhythmogenesis.

## Acknowledgments

This work was supported in part by the National Institutes of Health Grants RO1-HL58672, RO1-HL74854 and RO1-HL123093 (JYC); PO1-HL91799 (Project 2) and RO1-HL123093 (AMF); RO1-HL56025, RO1-HL61690, RO1-HL85503, PO1-HL-75443 and PO1-HL-91799 (WJK); RO1-HL-105414 (DGT); and RO1-HL123093 (JG & KK). Core facility services were provided by CNAC NIMH P30MH092177 at Temple University School of Medicine.

## References

1. Knezevic T, Myers VD, Gordon J, Tilley DG, Sharp TE 3rd, Wang J, et al. BAG3: a new player in the heart failure paradigm. Heart Fail Rev. 2015; 20:423–34. [PubMed: 25925243]
2. McCollum AK, Casagrande G, Kohn EC. Caught in the middle: the role of Bag3 in disease. Biochem J. 2010; 425:e1–3. [PubMed: 20001957]
3. Rosati A, Graziano V, De Laurenzi V, Pascale M, Turco MC. BAG3: a multifaceted protein that regulates major cell pathways. Cell death & disease. 2011; 2:e141. [PubMed: 21472004]
4. Ulbricht A, Hohfeld J. Tension-induced autophagy: may the chaperone be with you. Autophagy. 2013; 9:920–2. [PubMed: 23518596]
5. Pappas CT, Bhattacharya N, Cooper JA, Gregorio CC. Nebulin interacts with CapZ and regulates thin filament architecture within the Z-disc. Mol Biol Cell. 2008; 19:1837–47. [PubMed: 18272787]
6. Homma S, Iwasaki M, Shelton GD, Engvall E, Reed JC, Takayama S. BAG3 deficiency results in fulminant myopathy and early lethality. The American journal of pathology. 2006; 169:761–73. [PubMed: 16936253]
7. Odgerel Z, Sarkozy A, Lee HS, McKenna C, Rankin J, Straub V, et al. Inheritance patterns and phenotypic features of myofibrillar myopathy associated with a BAG3 mutation. Neuromuscular disorders : NMD. 2010; 20:438–42. [PubMed: 20605452]
8. Selcen D, Muntoni F, Burton BK, Pegoraro E, Sewry C, Bite AV, et al. Mutation in BAG3 causes severe dominant childhood muscular dystrophy. Annals of neurology. 2009; 65:83–9. [PubMed: 19085932]
9. Feldman AM, Begay RL, Knezevic T, Myers VD, Slavov DB, Zhu W, et al. Decreased levels of BAG3 in a family with a rare variant and in idiopathic dilated cardiomyopathy. Journal of cellular physiology. 2014; 229:1697–702. [PubMed: 24623017]
10. Norton N, Li D, Rieder MJ, Siegfried JD, Rampersaud E, Zuchner S, et al. Genome-wide studies of copy number variation and exome sequencing identify rare variants in BAG3 as a cause of dilated cardiomyopathy. American journal of human genetics. 2011; 88:273–82. [PubMed: 21353195]
11. Villard E, Perret C, Gary F, Proust C, Dilanian G, Hengstenberg C, et al. A genome-wide association study identifies two loci associated with heart failure due to dilated cardiomyopathy. European heart journal. 2011; 32:1065–76. [PubMed: 21459883]
12. Hishiya A, Kitazawa T, Takayama S. BAG3 and Hsc70 interact with actin capping protein CapZ to maintain myofibrillar integrity under mechanical stress. Circ Res. 2010; 107:1220–31. [PubMed: 20884878]

13. Franaszczyk M, Bilinska ZT, Sobieszczanska-Malek M, Michalak E, Sleszycka J, Sioma A, et al. The BAG3 gene variants in Polish patients with dilated cardiomyopathy: four novel mutations and a genotype-phenotype correlation. J Transl Med. 2014; 12:192. [PubMed: 25008357]
14. Jaffer F, Murphy SM, Scoto M, Healy E, Rossor AM, Brandner S, et al. BAG3 mutations: another cause of giant axonal neuropathy. J Peripher Nerv Syst. 2012; 17:210–6. [PubMed: 22734908]
15. Rosati A, Khalili K, Deshmane SL, Radhakrishnan S, Pascale M, Turco MC, et al. BAG3 protein regulates caspase-3 activation in HIV-1-infected human primary microglial cells. Journal of cellular physiology. 2009; 218:264–7. [PubMed: 18821563]
16. Zhou YY, Wang SQ, Zhu WZ, Chruscinski A, Kobilka BK, Ziman B, et al. Culture and adenoviral infection of adult mouse cardiac myocytes: methods for cellular genetic physiology. Am J Physiol Heart Circ Physiol. 2000; 279:H429–36. [PubMed: 10899083]
17. Tucker AL, Song J, Zhang XQ, Wang J, Ahlers BA, Carl LL, et al. Altered contractility and $[Ca^{2+}]_i$ homeostasis in phospholemman-deficient murine myocytes: Role of $Na^+/Ca^{2+}$ exchange. Am J Physiol Heart Circ Physiol. 2006; 291:H2199–H209. [PubMed: 16751288]
18. Grisanti LA, Talarico JA, Carter RL, Yu JE, Repas AA, Radcliffe SW, et al. β-adrenergic receptor-mediated transactivation of epidermal growth factor receptor decreases cardiomyocyte apoptosis through differential subcellular activation of ERK1/2 and Akt. J Mol Cell Cardiol. 2014; 72:39–51. [PubMed: 24566221]
19. Wang J, Gao E, Rabinowitz J, Song J, Zhang XQ, Koch WJ, et al. Regulation of in vivo cardiac contractility by phospholemman: role of $Na^+/Ca^{2+}$ exchange. Am J Physiol Heart Circ Physiol. 2011; 300:H859–68. [PubMed: 21193587]
20. Song J, Zhang XQ, Wang J, Cheskis E, Chan TO, Feldman AM, et al. Regulation of cardiac myocyte contractility by phospholemman:$Na^+/Ca^{2+}$ exchange vs. $Na^+$-$K^+$-ATPase. Am J Physiol Heart Circ Physiol. 2008; 295:H1615–H25. [PubMed: 18708446]
21. Song J, Gao E, Wang J, Zhang XQ, Chan TO, Koch WJ, et al. Constitutive overexpression of phospholemman S68E mutant results in arrhythmias, early mortality and heart failure: Potenial involvement of $Na^+/Ca^{2+}$ exchanger. Am J Physiol Heart Circ Physiol. 2012; 302:H770–H81. [PubMed: 22081699]
22. Wang J, Gao E, Song J, Zhang XQ, Li J, Koch WJ, et al. Phospholemman and β-adrenergic stimulation in the heart. Am J Physiol Heart Circ Physiol. 2010; 298:H807–15. [PubMed: 20008271]
23. Wang J, Chan TO, Zhang XQ, Gao E, Song J, Koch WJ, et al. Induced overexpression of $Na^+/Ca^{2+}$ exchanger transgene: Altered myocyte contractility, $[Ca^{2+}]_i$ transients, SR $Ca^{2+}$ contents and action potential duration. Am J Physiol Heart Circ Physiol. 2009; 297:H590–H601. [PubMed: 19525383]
24. Tadros GM, Zhang XQ, Song J, Carl LL, Rothblum LI, Tian Q, et al. Effects of $Na^+/Ca^{2+}$ exchanger downregulation on contractility and $[Ca^{2+}]_i$ transients in adult rat myocytes. Am J Physiol Heart Circ Physiol. 2002; 283:H1616–26. [PubMed: 12234816]
25. Mirza MA, Zhang XQ, Ahlers BA, Qureshi A, Carl LL, Song J, et al. Effects of phospholemman downregulation on contractility and $[Ca^{2+}]_i$ transients in adult rat cardiac myocytes. Am J Physiol Heart Circ Physiol. 2004; 286:H1322–30. [PubMed: 14684371]
26. Song J, Zhang XQ, Ahlers BA, Carl LL, Wang J, Rothblum LI, et al. Serine 68 of phospholemman is critical in modulation of contractility, $[Ca^{2+}]_i$ transients, and $Na^+/Ca^{2+}$ exchange in adult rat cardiac myocytes. Am J Physiol Heart Circ Physiol. 2005; 288:H2342–54. [PubMed: 15653756]
27. Zhang XQ, Ahlers BA, Tucker AL, Song J, Wang J, Moorman JR, et al. Phospholemman inhibition of the cardiac $Na^+/Ca^{2+}$ exchanger. Role of phosphorylation. J Biol Chem. 2006; 281:7784–92. [PubMed: 16434394]
28. Zhang XQ, Wang J, Song J, Rabinowitz J, Chen X, Houser SR, et al. Regulation of L-type calcium channel by phospholemman in cardiac myocytes. J Mol Cell Cardiol. 2015; 84:104–11. [PubMed: 25918050]
29. Zhang XQ, Ng YC, Moore RL, Musch TI, Cheung JY. In situ SR function in postinfarction myocytes. J Appl Physiol. 1999; 87:2143–50. [PubMed: 10601161]

30. Wang J, Song J, Gao E, Zhang XQ, Gu T, Yu D, et al. Induced overexpression of phospholemman S68E mutant improves cardiac contractility and mortality post-ischemia/reperfusion. Am J Physiol Heart Circ Physiol. 2014; 306:H1066–H77. [PubMed: 24486513]

31. Miller BA, Wang J, Hirschler-Laszkiewicz I, Gao E, Song J, Zhang XQ, et al. The second member of transient receptor potential-melastatin channel family protects hearts from ischemia-reperfusion injury. Am J Physiol Heart Circ Physiol. 2013; 304:H1010–22. [PubMed: 23376831]

32. Sweadner KJ, Rael E. The FXYD gene family of small ion transport regulators or channels: cDNA sequence, protein signature sequence, and expression. Genomics. 2000; 68:41–56. [PubMed: 10950925]

33. Zhang XQ, Qureshi A, Song J, Carl LL, Tian Q, Stahl RC, et al. Phospholemman modulates $Na^+/Ca^{2+}$ exchange in adult rat cardiac myocytes. Am J Physiol Heart Circ Physiol. 2003; 284:H225–33. [PubMed: 12388273]

34. Despa S, Bossuyt J, Han F, Ginsburg KS, Jia LG, Kutchai H, et al. Phospholemman-phosphorylation mediates the β-adrenergic effects on Na/K pump function in cardiac myocytes. Circ Res. 2005; 97:252–9. [PubMed: 16002746]

35. Cheung JY, Gordon J, Wang J, Song J, Zhang XQ, Tilley DG, et al. Cardiac dysfunction in HIV-1 transgenic mouse: Role of stress and BAG3. Clinical and translational science. 2015; 8:305–10. [PubMed: 26300236]

36. Ginsburg KS, Bers DM. Isoproterenol does not enhance Ca-dependent Na/Ca exchange current in intact rabbit ventricular myocytes. J Mol Cell Cardiol. 2005; 39:972–81. [PubMed: 16242149]

37. Lin X, Jo H, Sakakibara Y, Tambara K, Kim B, Komeda M, et al. β-adrenergic stimulation does not activate $Na^+$-$Ca^{2+}$ exchange current in guinea-pig, mouse and rat ventricular myocytes. Am J Physiol Cell Physiol. 2006; 290:C601–C8. [PubMed: 16207789]

38. Lee HC, Cherk SW, Chan SK, Wong S, Tong TW, Ho WS, et al. BAG3-related myofibrillar myopathy in a Chinese family. Clin Genet. 2012; 81:394–8. [PubMed: 21361913]

39. Wypijewski KJ, Howie J, Reilly L, Tulloch LB, Aughton KL, McLatchie LM, et al. A separate pool of cardiac phospholemman that does not regulate or associate with the sodium pump: multimers of phospholemman in ventricular muscle. J Biol Chem. 2013; 288:13808–20. [PubMed: 23532852]

40. De Marco M, Turco MC, Rosati A. BAG3 protein is induced during cardiomyoblast differentiation and modulates myogenin expression. Cell cycle. 2011; 10:850–2. [PubMed: 21311226]

41. Anderson ME. Why has it taken so long to learn what we still don't know? Circ Res. 2013; 113:840–2. [PubMed: 24030016]

## Highlights

1. Bcl2-associated athanogene 3(BAG3) is reduced in heart failure.
2. BAG3 is expressed on the sarcolemma and t-tubules of adult cardiac myocytes.
3. BAG3 associates with β1 adrenergic receptor, L-type $Ca^{2+}$ channel and phospholemman.
4. BAG3 downregulation by shRNA decreases contraction and $[Ca^{2+}]_i$ transient amplitudes in adult myocytes stimulated with isoproterenol.
5. BAG3 downregulation reduces L-type $Ca^{2+}$ current and sarcoplasmic reticulum $Ca^{2+}$ contents after isoproterenol.
6. BAG3 reduction prolongs action potential duration.

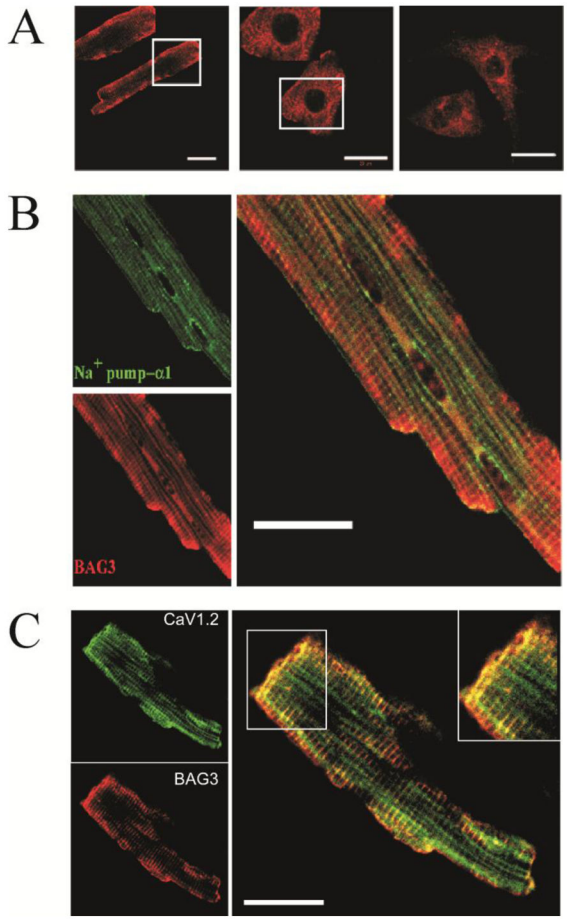


**Figure 1. BAG3 is expressed and co-localized with $Na^+$-$K^+$-ATPase and L-type $Ca^{2+}$ channel in the sarcolemma and t-tubules of adult mouse left ventricular (LV) myocytes**

(A). Confocal images of a freshly isolated adult WT mouse LV myocyte (left), neonatal rat ventricular myocyte (middle), and neonatal mouse ventricular myocyte (right) labeled with primary anti-BAG3 antibody are shown. Inset is an enlarged image of the area delineated by the white box. Scale bar = 20 μm. (B). Confocal images of a freshly isolated adult WT mouse LV myocytes labeled with anti-α1 subunit of $Na^+$-$K^+$-ATPase antibody (green) and anti-BAG3 antibody (red) are shown. Merged image demonstrates co-localization (orange) of BAG3 and $Na^+$-$K^+$-ATPase. Scale bar = 20 μm. (C). Confocal images of a freshly isolated adult WT mouse LV myocyte labeled with anti-α1c-$Ca_v$1.2 antibody (green) and anti-BAG3 antibody (red) are shown. Merged image demonstrates co-localization (orange) of BAG3 and $Ca_v$1.2. Inset is an enlarged image of the area delineated by the white box. Scale bar = 20 μm. For A, B and C, images from at least 5 myocytes were acquired.

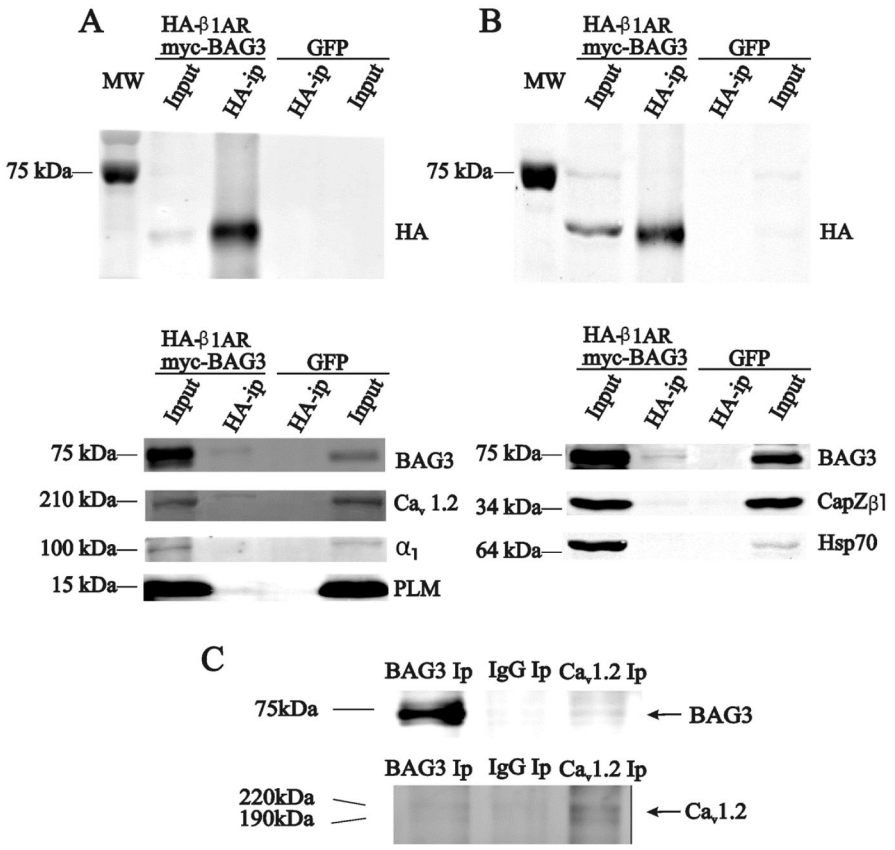


**Figure 2. BAG3 co-immunoprecipitates with β1AR and $Ca_V1.2$ but not α1-subunit of $Na^+$-$K^+$-ATPase in adult LV myocytes**

(A) & (B). WT myocytes infected with Adv-β1AR-HA + Adv-GFP-BAG3-myc or Adv-GFP were cultured for 48h. Immunoprecipitation (Methods) with anti-HA antibody was performed. Primary antibodies were used to identify BAG3, L-type $Ca^{2+}$ channel, $Na^+$ pump and phospholemman in one preparation (A) while association of β1AR-HA with BAG3, Capzβ1 and Hsp70 was tested in another preparation (B). Co-immunoprecipitation experiments were performed on 3 different myocyte preparations with similar results. (C). In non-infected WT myocytes, anti-BAG3 (left), non-immune rabbit IgG (middle) and anti-α1c-$Ca_V1.2$ (right) immunoprecipitates are probed for presence of $Ca_V1.2$ (bottom) or BAG3 (top), respectively.

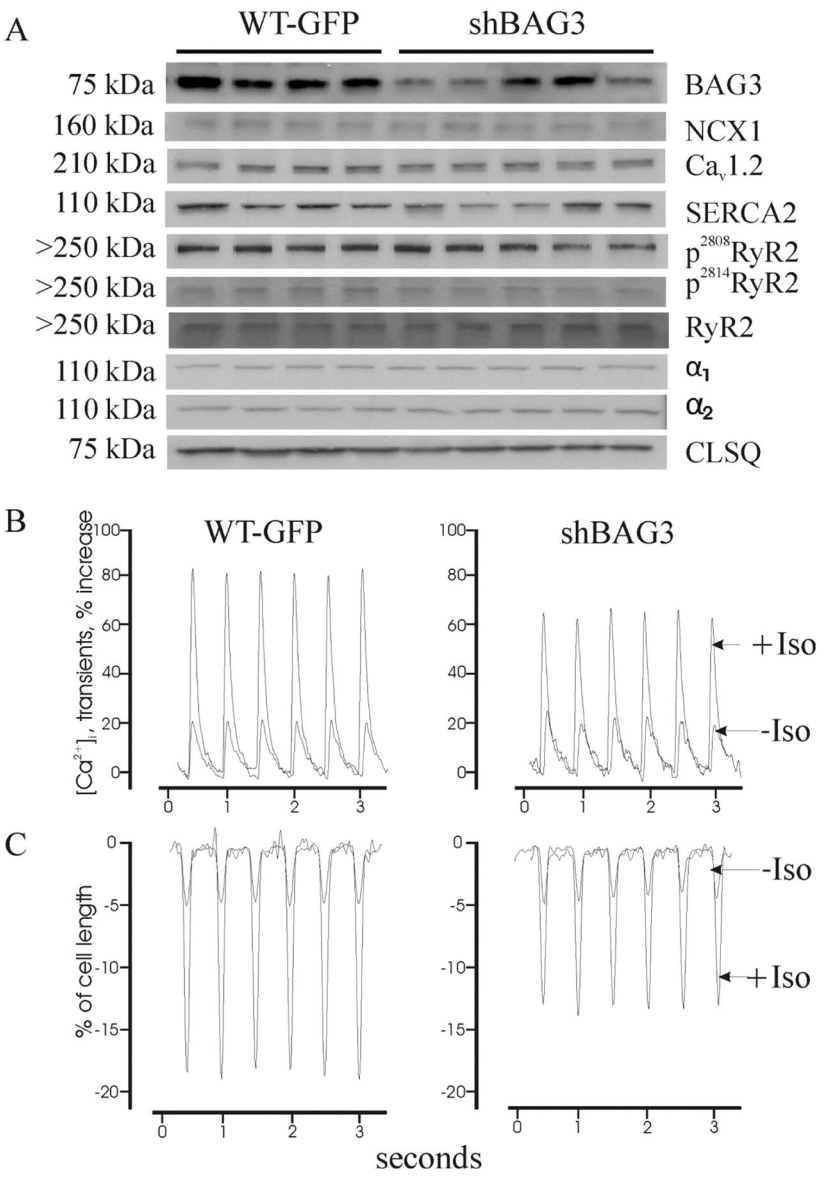


**Figure 3. BAG3 downregulation reduces contraction and $[Ca^{2+}]_i$ transient amplitudes in myocytes stimulated with isoproterenol**

(A). Adult mouse hearts were injected with Adv-shRNA-BAG3 + Adv-GFP or Adv-GFP alone, and tissues were harvested after 10 days and blotted for BAG3, $Na^+/Ca^{2+}$ exchanger (NCX1), α1c-subunit of L-type $Ca^{2+}$ channel ($Ca_v1.2$), sarco(endo)plasmic reticulum $Ca^{2+}$-ATPase (SERCA2), cardiac ryanodine receptor phosphorylated at serine$^{2808}$ and at serine$^{2814}$ ($p^{2808}$RyR2 and $p^{2814}$RyR2), total RyR2, α1- and α-2subunits of $Na^+$-$K^+$-ATPase, and calsequestrin (CLSQ) was used as loading control. Quantitative results are shown in Table 1. (B & C). Representative traces of $[Ca^{2+}]_i$ transients (B) and cell shortening (C) in GFP and shBAG3 myocytes, before and after addition of isoproterenol (1 μM). Composite results are shown in Table 2.

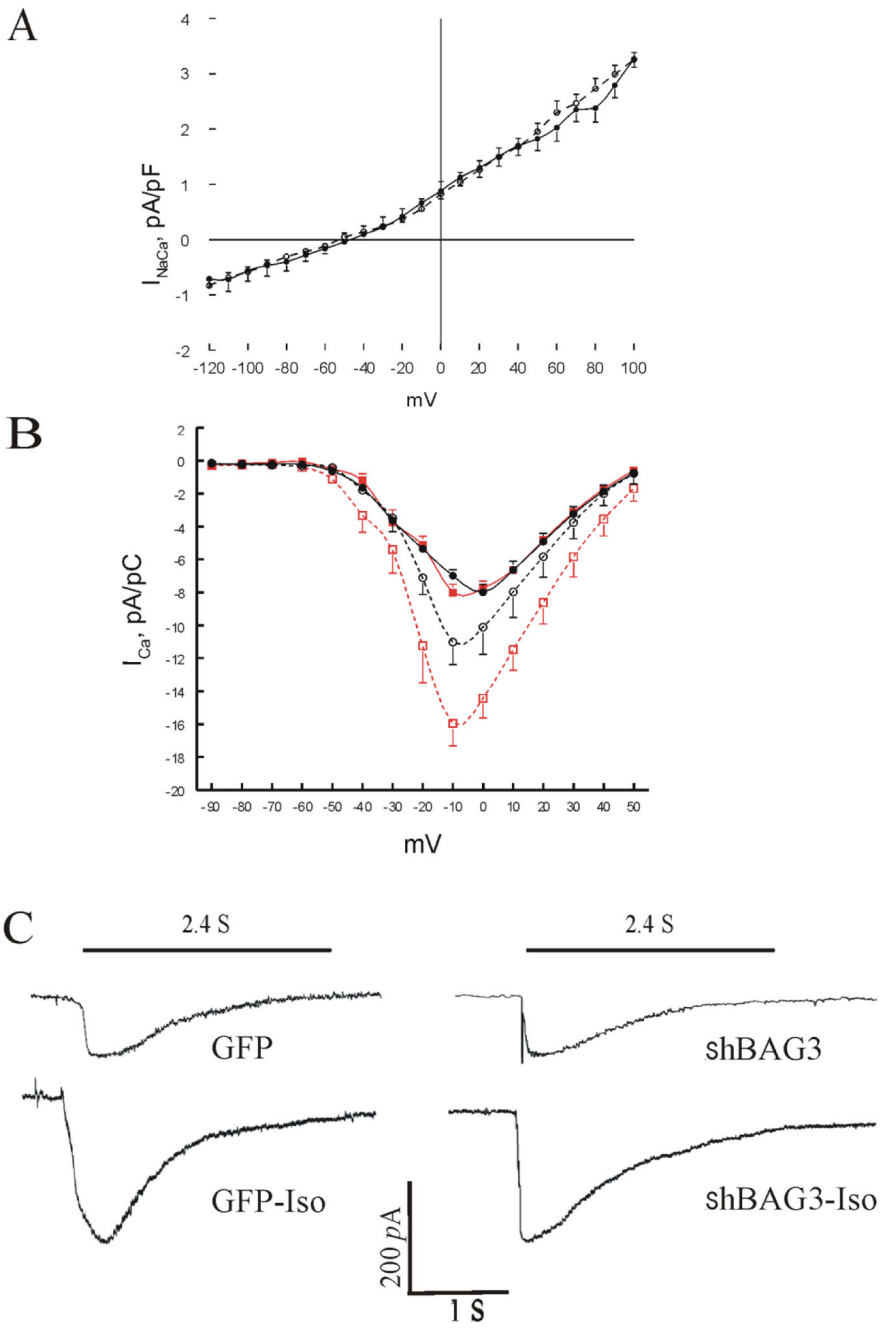


**Figure 4. BAG3 downregulation reduces $I_{Ca}$ and SR $Ca^{2+}$ contents but has no effect on $I_{NaCa}$**

(A). $I_{NaCa}$ in GFP myocytes (○; n=6 myocytes from 2 mice) or shBAG3 (●; n=5 myocytes from 2 mice) myocytes are shown. (B). $I_{Ca}$ in GFP (■, before Iso; □, after Iso; n=5 myocytes from 3 mice) and shBAG3 (●, before Iso; ○, after Iso; n=8 myocytes from 5 mice) myocytes are shown. (C). Representative $I_{NaCa}$ traces from GFP and shBAG3 myocytes after caffeine (5 mM) exposure. The $I_{NaCa}$ time integral is an estimate of SR $Ca^{2+}$ content. Composite results are shown in Table 2.

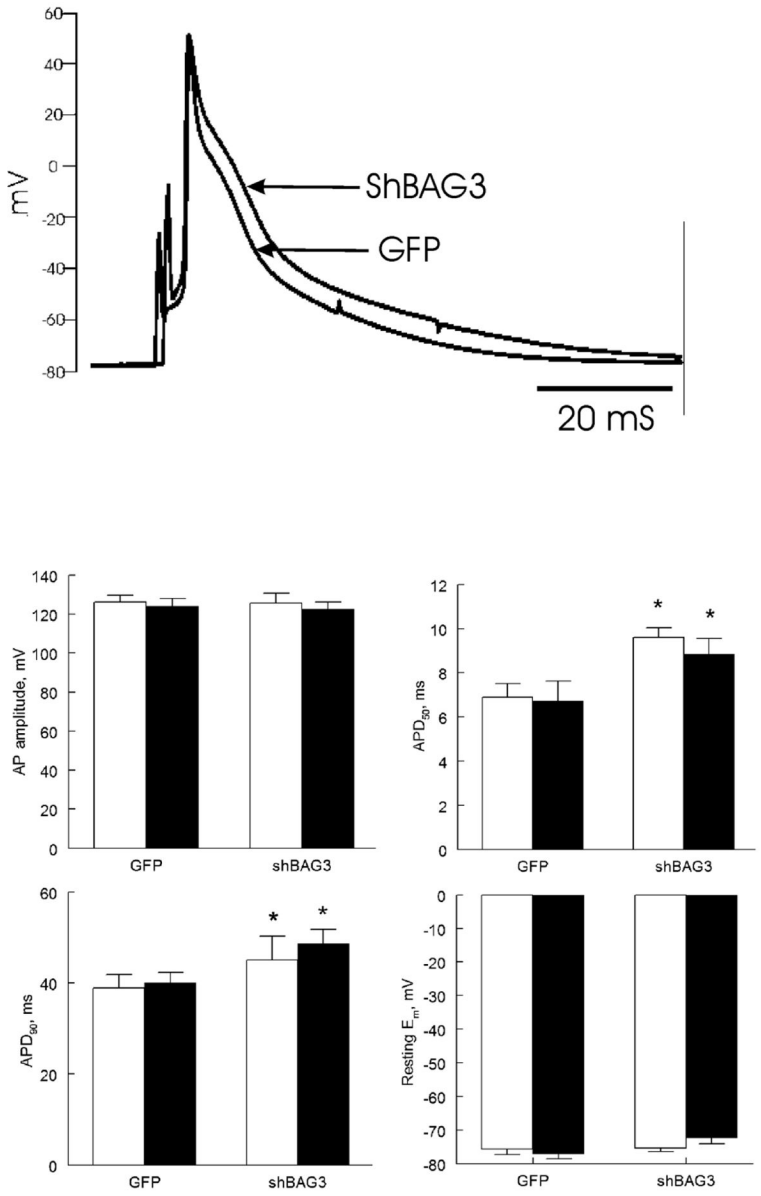


**Figure 5. BAG3 downregulation prolongs action potential duration (APD)**

(A). Representative action potentials of GFP and shBAG3 myocytes are shown. (B). Means ± SE of resting membrane potential ($E_m$), action potential amplitude, and APD at 50% ($APD_{50}$) and 90% repolarization ($APD_{90}$) from 7 GFP (3 mice) and 5 shBAG3 myocytes (3 mice), both before (open bars) and after (filled bars) 1 μM Iso are shown. *p<0.045; GFP vs. shBAG3.

## Table 1

Effects of BAG3 downregulation on levels of selected proteins

| | GFP (4) | shBAG3 (5) |
|---|---|---|
| BAG3 | 2.651 ± 0.558 | 1.211 ± 0.224* |
| NCX1 | 0.076 ± 0.019 | 0.086 ± 0.015 |
| $Ca_v1.2$ | 0.228 ± 0.008 | 0.216 ± 0.011 |
| SERCA2 | 0.918 ± 0.173 | 0.877 ± 0.152 |
| $p^{2808}$RyR2 | 0.527 ± 0.036 | 0.508 ± 0.036 |
| $p^{2814}$RyR2 | 0.107 ± 0.023 | 0.104 ± 0.027 |
| RyR2 | 0.204 ± 0.066 | 0.216 ± 0.020 |
| $\alpha_1$-subunit, $Na^+$-$K^+$-ATPase | 0.170 ± 0.002 | 0.173 ± 0.003 |
| $\alpha_2$-subunit, $Na^+$-$K^+$-ATPase | 0.045 ± 0.003 | 0.047 ± 0.001 |

Values (in arbitrary units) are means ± SE of protein band intensities normalized to respective calsequestrin loading controls. Adv-GFP or Adv-shRNA BAG3 + Adv-GFP was injected into LV of WT mice. Homogenates were obtained from green fluorescent LV slices 10 days post-injection (Methods). Number of hearts is given in parentheses. BAG3, Bcl2-associated athanogene 3; $Ca_V1.2$, $\alpha_{1C}$-subunit of L-type $Ca^{2+}$ channel; GFP, green fluorescent protein; NCX1, cardiac $Na^+/Ca^{2+}$ exchanger; $p^{2808}$RyR2 and $p^{2814}$RyR2, cardiac ryanodine receptor phosphorylated at $Ser^{2808}$ and $Ser^{2814}$, respectively; RyR2, total RyR2; SERCA2, sarco(endo)plasmic reticulum $Ca^{2+}$-ATPase; shRNA, short hairpin RNA.

*$p<0.045$, GFP vs. shRNA-BAG3

## Table 2

Effects of LV-injected shBAG3 on single myocyte contraction and $[Ca^{2+}]_i$ dynamics

| | Iso | GFP | shBAG3 |
|---|---|---|---|
| Maximal contraction amplitude, % | − | 5.52 ± 0.45 (12/4) | 5.74 ± 0.49 (11/4) |
| | + | 17.92 ± 0.47 | 15.18 ± 0.73* |
| $[Ca^{2+}]_i$ transient amplitude, % | − | 20.2 ± 1.6 (14/3) | 18.7 ± 1.7 (14/3) |
| | + | 81.6 ± 5.1 | 64.7 ± 4.1* |
| $t_{1/2}$ of $[Ca^{2+}]_i$ transient decline, ms | − | 117 ± 6 (14/3) | 121 ± 7 (14/3) |
| | + | 72 ± 4 | 83 ± 3 |
| SR $Ca^{2+}$ content, fM/fF | − | 7.3 ± 0.6 (5/3) | 6.7 ± 0.1 (6/3) |
| | + | 21.2 ± 1.3 | 19.5 ± 0.7+ |
| $t_{1/2}$ of $I_{NaCa}$ decline, ms | − | 927 ± 65 (5/3) | 887 ± 248 (6/3) |
| | + | 782 ± 186 | 929 ± 161 |

Values are means ± SE. Numbers (x/y) in parentheses are numbers of myocytes (x) isolated from numbers of mice (y). Adv-GFP or Adv-GFP + Adv-shRNA- BAG3 was injected into LV of WT mice and myocytes were isolated from the green fluorescent portions of the LV 10 days post-injection (Methods). Contraction amplitudes and $[Ca^{2+}]_i$ transients were measured at 1.8 mM $[Ca^{2+}]_o$, 2 Hz, 37°C. Contraction amplitudes are given in % resting cell length; $[Ca^{2+}]_i$ transient amplitudes are in % increase in fura-2 signal.

* $p<0.03$ (group x Iso interaction effect);

+ $p<0.05$ (group effect).

## Table 3

Effects of isoproterenol, forskolin and dibutryl cAMP on maximal $I_{Ca}$ amplitude

| | Drug | GFP | shBAG3 |
|---|---|---|---|
| 1μM isoproterenol | − | 8.03 ± 0.53 (5/3) | 6.98 ± 0.36 (8/5) |
| | + | 15.96 ± 1.35 | 11.02 ± 1.36* |
| 10 μM forskolin | − | 6.66 ± 0.82 (4/2) | 6.88 ± 0.36 (7/5) |
| | + | 13.32 ± 1.00 | 13.13 ± 0.41# |
| 5 mM DBcAMP | − | 7.73 ± 0.28 (3/1) | 7.26 ± 0.60 (6/3) |
| | + | 14.39 ± 0.08 | 14.85 ± 0.72# |

Values are means ± SE of $I_{Ca}$ amplitudes measured at −10 mV. Numbers (x/y) in parentheses are numbers of myocytes (x) isolated from numbers of mice (y).

* $p<0.02$, GFP vs. shBAG3;

# $p<0.02$, shBAG3-Iso vs. shBAG3-forskolin or shBAG3-DBcAMP.